UDC 621.77:519.61
Preliminary communication
Received: 11.12.2009.

Finite element analysis of open die extrusion of Al-5Zn-1Mg alloy

K. Geethalakshmi[(1)] and **K. Srinivasan**[(2)]
[(1)]Padre Conceicao College of Engineering, Angel Ashram, Verna, Goa - 403722, INDIA
e-mail: geethashyam@gmail.com
[(2)]Department of Metallurgical & Materials Engineering, National Institute of Technology Karnataka, Suratkal - 574157, INDIA, e-mail: ksrini@nitk.ac.in & ksrini@krec.ac.in

SUMMARY

In this work, an effort has been made to study the open die extrusion of Al-5Zn-1Mg alloy using finite element analysis. The two basic parameters of open die extrusion, i.e., die included angle and the extrusion strain are varied to find the corresponding limiting strain values. Effect of main parameters on the open die extrusion is analyzed, and the limiting range of deformation is obtained. The results obtained are verified by means of contrasting with the experimental data. Pure open die extrusion is found to be possible for extrusion strain (relative strain during extrusion) up to 0.28. However, as the extrusion strain increases from 0.09 to 0.28, upsetting dominates over pure extrusion on varying the die angle from 12° to 40°.

Key words: *open die extrusion, die angle, extrusion strain, Al-5Zn-1Mg alloy, limiting strain.*

1. INTRODUCTION

Over the years, age-hardenable, high-strength aluminium alloys belonging to the Al-Zn-Mg family have proved useful as structural materials. Their usefulness in airframe structures such as aircraft, space vehicles and lightweight armoured carriers has been critical to vehicle performance on account of their superior performance in many aspects, including high strength-to-weight ratio, attractive specific stiffness, low cost, durability, machinability and good formability [1-2].

Open die extrusion is considered to be a process in which a short billet is pushed through a narrow opening in a conical die that determines the cross section of the final product [3]. The schematic set up for open die extrusion is shown in Figure 1.

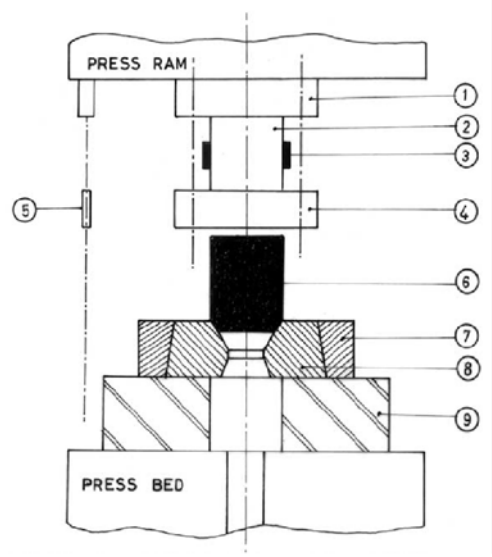

1. Hard Plate, 2. Load Cell, 3. Strain Gauges, 4. Punch, 5. LVDT, 6. Billet, 7. Die, 8. Shrink Ring, 9. Bolster

Fig. 1 Schematic set up for open die extrusion

The geometry of the operation is described by the semicone angle, the reduction ratio and the initial aspect ratio. The relevant material characteristics are the shear flow stress and the friction factor. In this operation, the reduction is limited as the allowable driving force is limited. When the punch pressure for extrusion equals the yield stress of the material, upsetting of the billet above the die will take place, rather than extrusion of billet through the die.

In conventional extrusion, the force rises rapidly to its peak value initially as the billet is upset, and then decreases, and "steady state" extrusion proceeds and finally reaches its minimum value followed by a sharp rise as the "discard" is compacted whereas in open die extrusion, after an initial rise the force remains constant if there is a pure extrusion. If upsetting takes place, force continuously increases with increasing movement of ram with a slope change at the point where upsetting starts. The change in slope distinguishes between the initial die filling and upsetting regions.

Open die extrusion is expected to eliminate the friction component of the container and thus the total force consists of three terms only, i.e., ideal force, shear force and die friction force as the container wall billet friction is absent. The load or pressure-displacement curves for conventional extrusion and open die extrusion are shown in Figure 2.

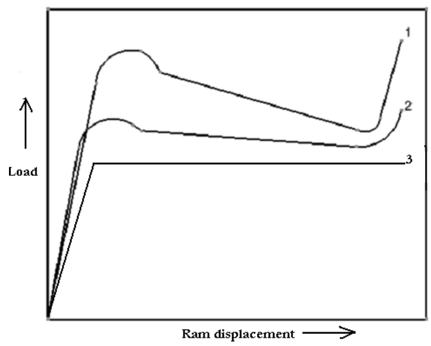

Fig. 2 Load vs. displacement curves for forward (curve 1) & backward (curve 2) conventional extrusion and open die extrusion (curve 3)

When the punch pressure for extrusion equals the yield stress for a particular extrusion, that strain is called the limiting strain. If the punch pressure exceeds the yield stress, upsetting of the billet above the die will dominate rather than extrusion of billet through the die [4]. There is an optimum angle at which the punch pressure and force are minimum for containerless extrusion. This angle is called optimum die angle and it depends on extrusion strain and friction factor of the material.

The absence of container - billet frictional force component of the overall force for extrusion ensures that the force required is considerably less and lubrication requirement is also reduced in open die extrusion. Hence lower capacity presses will be sufficient and tooling material requirements are less critical in open die extrusion.

The disadvantage of this technique is seen in terms of difficulties in achieving greater strains, and in handling greater ratios of billet length to diameter, per push. The possibility of buckling or upsetting of the unsupported billet for greater strains forms another limitation of this technique. Therefore open die extrusion can be economical, feasible and effectively employed only for short components and smaller strains in a single pass.

The Al-Zn-Mg system offers the greatest potential of all aluminium alloys for age-hardening. Compositions within this system have the highest known strength of all commercial aluminium alloys. The high strength is due to precipitation of $MgZn_2$ particles. The most widely used alloy contains approximately *4.5%* Zn and *1.3%* Mg. With respect to composition, both tensile strength and susceptibility to cracking increases as the Zn + Mg content increases [5]. Keeping in view of these points Al-5Zn-1Mg alloy was taken for the present work.

Finite Element Method (FEM) is a very powerful technique for determining the distribution of stresses and strains in plane stress, plane strain, and axisymmetric conditions for both steady-state and non-steady state deformation problems [6-8]. FEM analysis can be used to simulate deformation very effectively when combined with real time computer graphics output. Finite Complex problems can be modeled with relative ease; several alternative configurations can be tried out on a computer before the first prototype is built [9].

ANSYS program has a comprehensive graphical user interface that gives the user easy, interactive access to program functions, commands, documentation and reference material. It has capabilities ranging from a simple, linear static analysis to a complex nonlinear transient dynamic analysis. ANSYS has a number of inbuilt material models which are developed on the basis of wide accepted theory related to each material.

2. FINITE ELEMENT ANALYSIS OF OPEN DIE EXTRUSION

2.1 Problem statement

It is required to generate the grid deformation during open die extrusion of the billet, carried out at room temperature. Upsetting of the billet, which occurs just above limiting strain of the extrusion process, is used as the criteria to predict limiting strain for a given conical die of die angle 2α. In order to eliminate the problem of buckling of the billet, the height to diameter ratio is kept at *1.5* for all the cases. Finite element analysis software, ANSYS 10.0 is used to formulate, to solve and to analyse the results. Two dimensional formulations are chosen as the extrusion billet and die are of axisymmetric shape. In brief, the physical process is formulated as a rectangular cross section of the billet being pushed through conical die, at a constant strain rate and friction factor.

Many previous works on finite element modeling and analysis of cold forward extrusion process are taken as a basis to formulate the present problem [10-14]. The geometrical dimensions are listed as follows:

- geometrical: height of the billet (h) = *37.5 mm*, diameter of the billet (d) = *25 mm*.
- die used: conical dies with die angle *12°*, *15°*, *25°*, *30°* and *40°* having a land of *4 mm*.

The material properties of Al-5Zn-1Mg alloy considered for the finite element analysis are as follows:

- density: *2.7 g/cm³*
- yield strength: *190 MPa*
- Young's modulus: *76 GPa*
- coefficient of friction: *0.25*

For 2-D modeling of solid structures element PLANE 182 is used. This element can be used as either a plane element or an axisymmetric element. It is defined by four nodes having two degrees of freedom at each node: translations in the nodal x and y directions. The element has plasticity, hyperelasticity, stress stiffening, large deflection, and large strain capabilities. It also has mixed formulation capability for simulating deformations of nearly incompressible elastoplastic materials, and fully incompressible hyperelastic materials. Element formulation is selected as pure displacement type, since it is suitable for elastoplastic formulation.

Material properties, namely, Young's modulus, Poisson's ratio and density of the material are assigned. Among the available material nonlinearity models, Bilinear Isotropic Hardening Option (BISO) is selected and assigned for this analysis. BISO option uses the von Mises yield criteria coupled with an isotropic work hardening assumption. This model represents rate-independent plasticity. The material behavior is described by a bilinear stress-strain curve starting at the origin with positive stress and strain values. The initial slope of the curve is taken as the elastic modulus of the material.

2.2 Meshing

ANSYS provides two types of finite element meshing methods. They are free meshing and mapped method. In free meshing method, user does not have the control on the element size. Mapped meshing has control over the element size throughout the meshing area thereby ensuring uniform meshing throughout the area. Hence mapped meshing has been chosen for the present work. The rectangular area of the billet and conical die has to be meshed with suitable elements. Plane 182 element is chosen to mesh the billet.

2.3 Generating contact pairs

To model the interaction between die surface-billet material contact technology is used. Contact problems fall into two general classes: rigid-to-flexible and flexible-to-flexible. In rigid-to-flexible contact problems, one or more of the contacting surfaces are treated as rigid. Many metal forming problems fall into this category. The other class, flexible-to-flexible, both (or all) contacting bodies are deformable. For the present work rigid-to-flexible contact pair is selected. Die surface is made rigid, where as billet material is treated as flexible. The contact elements used are TARGE 169 and CONTA 171.

TARGE 169 is used to represent various 2-D "target" surfaces for the associated contact elements. The contact elements themselves overlay the solid elements describing the boundary of a deformable body and are potentially in contact with the target surface, defined by TARGE 169. This target surface is discretized by a set of target segment elements and is paired with its associated contact surface via a shared real constant set. We can impose any translational or rotational displacement, temperature, voltage, and magnetic potential on the target segment element. We can also impose forces and moments on target elements.

CONTA 171 is used to represent contact and sliding between 2-D "target" surfaces and a deformable surface, defined by this element. The element is applicable to 2-D structural and coupled field contact analyses. This element is located on the surfaces of 2-D solid, shell, or beam elements without mid side nodes. It has the same geometric characteristics as the solid, shell, or beam element face with which it is connected. Contact occurs when the element surface penetrates one of the target segment elements on a specified target surface. CONTA 171 input data applicable to present work include material property such as coefficient of friction as mentioned in the materials property details. There are two degrees of freedom in x and y directions for each node. The correct node ordering of the contact element is critical for proper detection of contact. The nodes must be ordered such that the target must lie to the right side of the contact element when moving from the first contact element node to the second contact element.

Due to planar representation of the billet, there will be line contact between die and billet. Two contact pairs are identified in the present formulation.

First contact pair: Elements at the top edge of the rectangle billet overlaid with CONTA 171 and a line (located on the top edge of the rectangle) meshed with TARGE 169 forms the first contact pair. The rigid target surface can be associated with a "pilot node," which is really an element with one node, whose motion governs the motion of the entire target surface. We can think of a pilot node as a handle for the rigid target surface. Forces/moments or rotations/ displacements for the entire target surface can be prescribed on just the pilot node. The pilot node can be one of the nodes on the target element or a node at any arbitrary location. The location of the pilot node is important only when rotation or moment loading is required. If we define a pilot node, ANSYS checks for boundary conditions only on the pilot node and ignores any constraints on other nodes. In the present work, pilot node is located *10 mm* (arbitrary value) above the billet top surface. This rigid target surface with pilot node is used to give the downward displacement to the billet in order to push it through the conical die. In other words, the pushing of the billet through die is achieved through pilot node movement.

Second contact pair: The conical surface of die, which comes into contact with the right vertical surface of the billet forms second contact pair. The conical die surface is meshed with TARGE 169 elements, which form the rigid target surfaces. The element associated with right vertical edges of the rectangle billet is overlaid with CONTA 171 elements and they form the flexible contact surfaces.

2.4 Applying boundary conditions

In this step, degrees of freedom constraints, loads and displacements at the desired nodal points are defined. Present formulation involves degrees of freedom constraints and pilot node displacements only.

Translation in the *x*-direction and rotation of the pilot node (corresponding to the first contact pair) are constrained and it is having translatory movement in *y*-direction. This movement is required to apply the vertical displacement to the billet. All the nodes of the elements of the target surfaces associated with die surfaces are constrained for *x* and *y* translatory motion as well as rotation. This is to ensure the fixed condition of the die during extrusion. A sample meshed model with degrees of freedom constraints is shown in Figure 3.

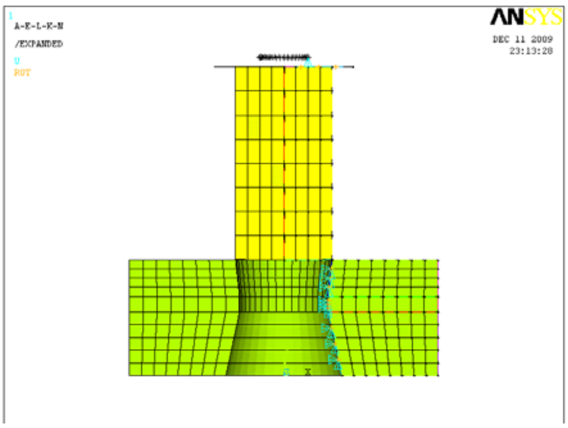

Fig. 3 Meshed model with degrees of freedom constraints

2.5 Solving

After all the preprocessing steps described above are finished, the problem is ready for solving. Due to the large strains involved, material non-linearity and contact surfaces involved in the problem, our solution will be non-linear, static type.

2.6 Post processing

Post processing means reviewing the results of an analysis. Two postprocessors are available to review the results: POST1, the general postprocessor, and POST26, the time-history postprocessor (used for analysis of time dependent results). POST1 allows us to review the results over the entire model at specific load steps and substeps. POST1 has many capabilities, ranging from simple graphics displays and tabular listings to more complex data manipulations such as load case combinations. In the present work, graphical display of results is used for viewing the results.

In each case, the billet is pushed through die until full length of the billet enters the die. This will ensure free extrusion. If upsetting is encountered, the billet cannot be pushed through its full length.

3. RESULTS AND DISCUSSION

Finite element models of the process, with die angle and extrusion strain as variable parameters are solved. ANSYS commands are used for the analysis of extrusion through dies of die angle *15°*, *20°*, *25°*, *30°*, *35°* and *40°*. Commands used to generate the geometrical model of the die are modified, while using for different dies and extrusion strains. Vertical movement of pilot node is used to push the billet through die. At the limiting extrusion strain simple upsetting of the billet above the die is observed. The grid deformations of the analysis carried out are presented below in Figures 4 to 7.

From Figures 4 to 7, we can see that at *0.09* extrusion strain, pure open die extrusion takes place for all die angles from *12°* to *30°* and at *0.13* extrusion strain, upsetting occurs along with extrusion for *25°* die angle and for *30°* die angle upsetting is found to take place rather than pure extrusion. As the strain is increased further, upsetting dominates over extrusion and at *0.21* strain, open die extrusion is possible only at die angle of *25°* where as for all other die angles upsetting is found to the more favourable than pure extrusion.

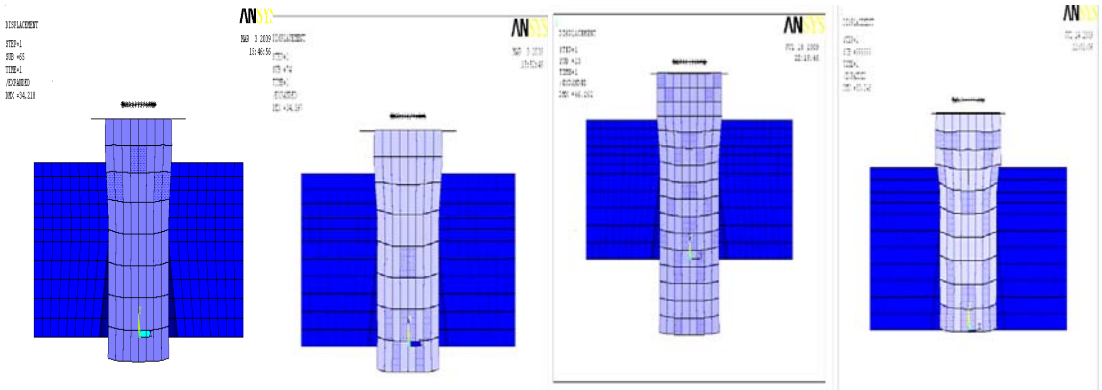

(a) (b) (c) (d)

Fig. 4 The grid deformations at extrusion strain of 0.09 for die angles of (a) 12°, (b) 15°, (c) 25° and (d) 30°

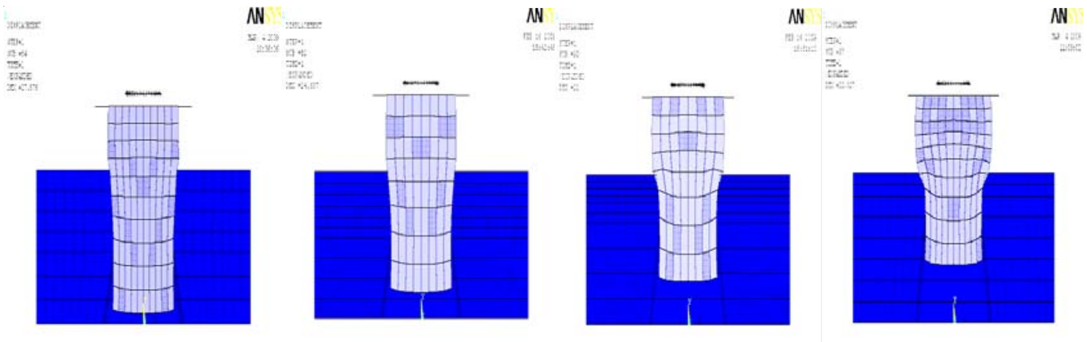

(a) (b) (c) (d)

Fig. 5 The grid deformations at extrusion strain of 0.13 for die angles of (a) 12°, (b) 15°, (c) 25° and (d) 30°

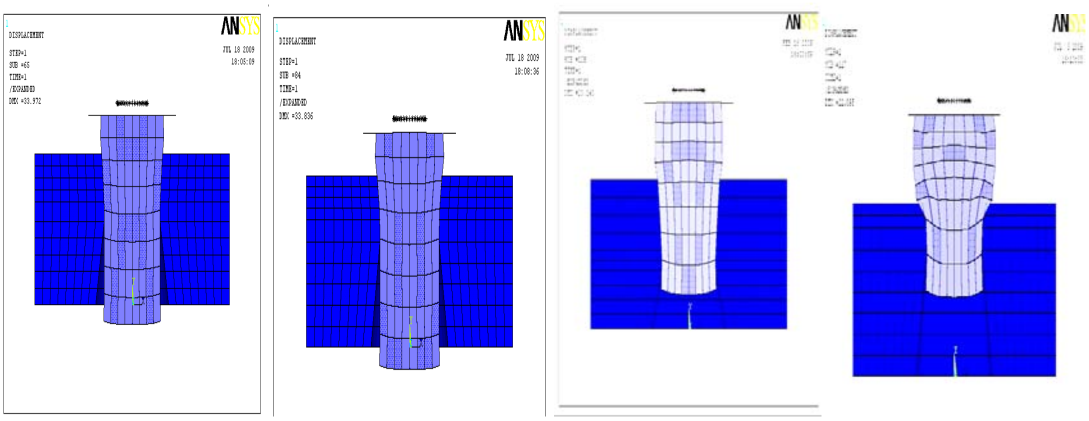

(a) (b) (c) (d)

Fig. 6 The grid deformations at extrusion strain of 0.18 for die angles of (a) 12°, (b) 15°, (c) 25° and (d) 30°

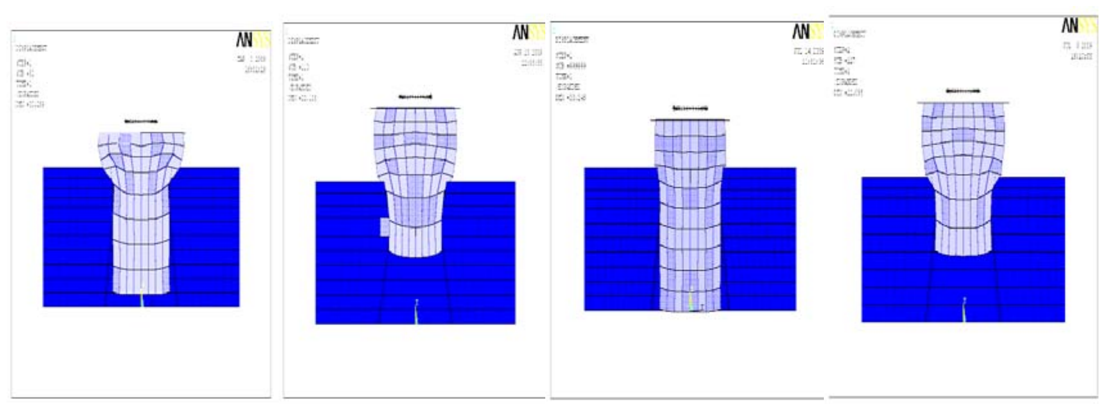

(a) (b) (c) (d)

Fig. 7 The grid deformations at extrusion strain of 0.21 for die angles of (a) 12°, (b) 15°, (c) 25° and (d) 30°

In order to validate the results obtained, aluminium, zinc and magnesium were weighed in the required proportion, melted and cast into billets and then machined into testing samples of diameter *25 mm* and height *37.5 mm*. The samples were then annealed at *400° C* for *1 hr*. Conical dies of included angles *12°*, *15°*, *25°*, *30°* and *40°* for strains of *0.09*, *0.13*, *0.18*, *0.21* and *0.28* were made from high carbon high chromium steel. The design of a typical extrusion die is shown in Figure 8.

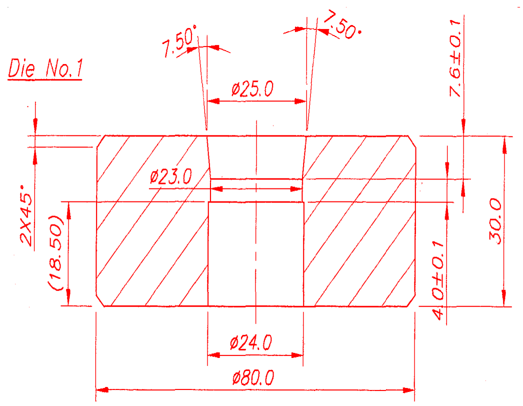

Fig. 8 Design of a typical extrusion die

The test samples were then extruded through the conical dies at room temperature using a Universal Testing Machine of *40 T* capacity using graphite powder as lubricant. The force – stroke data was noted down. The force - stroke diagrams for *0.09*, *0.13* and *0.21* extrusion strains are shown in Figure 9.

(a)

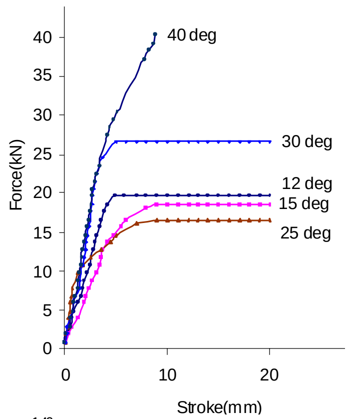

(b)

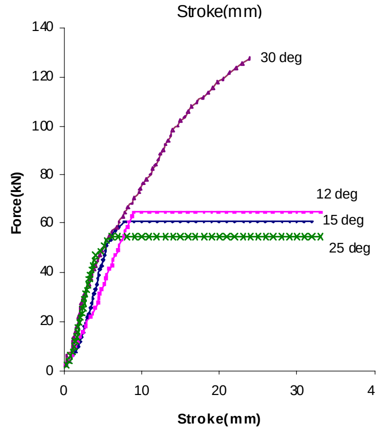

(c)

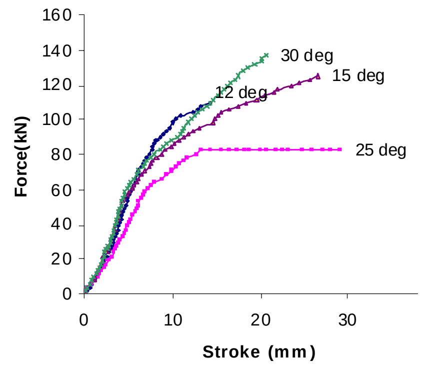

Fig. 9 Force – Stroke diagram for open die extrusion at (a) 0.09 strain, (b) 0.13 strain and (c) 0.21 strain

Figure (9a) shows that for die angles of *12°*, *15°*, *25°* and *30°*, the force remains constant at some particular point indicating the pure extrusion process, where as for *40°* die angle, the force increases with increasing movement of ram with a change of slope. So we can clearly see that, pure extrusion takes place for all die angles except *40°*. Of all the die angles for which pure extrusion is possible, *25°* die angle shows the minimum in force required for extrusion. This shows that *25°* is the optimum die angle for open die extrusion at *0.09* strain. However, as the extrusion strain increases, the force remains constant only at some particular die angles. The results show similar trend as in finite element analysis.

The maximum load divided by the area of cross section of the billet under the punch is considered as the actual punch pressure. The punch pressure for pure extrusion for all the die angles and strains under consideration are calculated and the dependence of experimental punch pressure on extrusion strain is shown in Figure 10.

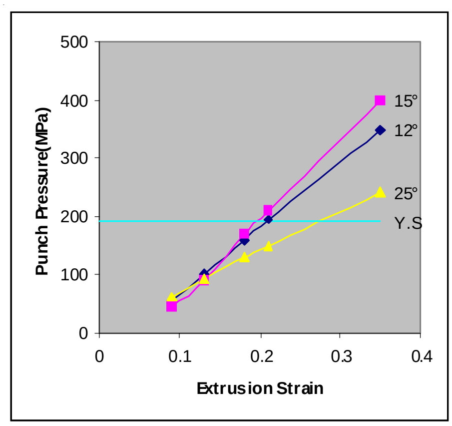

Fig. 10 Variation of experimental punch pressure with extrusion strain

Figure 10 shows that punch pressure is much less than the yield stress up to *0.21* extrusion strain at *25°* die angle and maximum deformation is possible at this die angle, as the extrusion strain has the highest value at this die angle. For *12°* and *15°* die angle, the maximum strain is considerably less as compared to *25°* and hence we can say that open die extrusion is most favourable at particular die angle.

The results of the open die extrusion experiment was compared with the results obtained in finite element analysis. The comparison of limiting strain values from experimental analysis and finite element analysis is shown in Table 1.

Table 1. Comparison of limiting strain values of experimental analysis and finite element analysis

Die included angle (deg)	*Limiting strain*	
	FEA	*Experimental*
12	*0.21*	*0.22*
15	*0.18*	*0.19*
25	*0.21*	*0.28*

From the results obtained it can be seen that for extrusion strain of *0.09* pure extrusion was possible for all die all angles from *12°* to *30°*. But as the extrusion strain was increased, upsetting was found to dominate over pure extrusion. Considering all the die angles, as the extrusion strain was increased from *0.09* to *0.28*, the punch pressure was found to increase from around *50 MPa* to *300 MPa*. However, upsetting was observed at extrusions strains of above *0.21* depending on die angle. Hence, from the dependence of punch pressure on extrusion strain and die angle, it can be seen that punch pressure increases as the extrusion strain increases.

It is evident that the results of the experimental analysis and finite element analysis show the same trend. However, the punch pressure values obtained in the finite element analysis was found to be on the higher side as compared to experimental ones. This is because of the fact that the flow stress values of the material reduces during actual deformation in the experimental analysis due to temperature rise in the deformation zone as a consequence of adiabatic and frictional heating.

4. CONCLUSIONS

On the basis of the numerical and experimental results several statements could be formulated:

1. For strain value of *0.09*, pure extrusion takes place for die all angles from *12°* to *30°*.
2. For higher strain values, pure extrusion takes place over a narrow range of lower die angles.
3. As the extrusion strain increases, upsetting dominates over pure extrusion.
4. The punch pressure values obtained in the experimental analysis were found to be on the lower side as compared to the finite element analysis, which is attributed to the increase in temperature due to adiabatic and friction heating in the deformation zone.

5. REFERENCES

[1] J.T. Staley, *Microstructure and Toughness of High Strength Aluminum Alloys*, ASTM STP 304, American Society for Testing Materials, Philadelphia, 1976.

[2] J.T. Staley, History of wrought-aluminum-alloy development, In: Aluminum Alloys: Contemporary Research and Applications, Eds. A.K. Vasudevan and R.D. Doherty, Academic Press, Boston, pp. 3-31, 1989.

[3] B. Avitzur, *Metal Forming: Processes and Analysis*, Tata McGraw Hill, New Delhi, pp. 229-234, 1977.

[4] K. Srinivasan and P. Venugopal, Direct and inverted open die extrusion of rods and tubes, *Journal of Materials Processing Technology*, Vols. 153-154, pp. 765-770, 2004.

[5] I.J. Polmear, *Light Alloys: Metallurgy of Light Metals*, Arnold Publication, 3rd edition, pp. 115-118, 1995.

[6] C.S. Desai and J.F. Abel, *Introduction to Finite Element Method*, Van Nostrand Reinhold, New York, pp. 248-249, 1972.

[7] O.C. Zienkiewicz, *The Finite Element Method*, 3rd edition, McGraw Hill, New York, pp. 25-53, 1993.

[8] O.C. Zienkiewicz and R.L. Taylor, *The Finite Element Method - Volume 2*, 3rd edition, McGraw Hill, New York, pp. 1-26, 1993.

[9] H. Sofuoglu and H. Gedikli, Physical and numerical analysis of three dimensional extrusion process, *Computational Materials Science*, Vol. 31, pp. 113-124, 2004.

[10] K. Srinivasan and P. Venugopal, Adiabatic and friction heating on the open die extrusion of solid and hollow bodies, *Journal of Materials Processing Technology*, Vol. 70, pp. 170-177, 1997.

[11] M. Gierzynska-Dolna and P. Lacki, Some aspects of modeling of metal forming processes, *Computers and Structures*, Vol. 81, pp. 605-613, 2003.

[12] A.F.M. Arif, On the use of non-linear finite element analysis in deformation evaluation and development of design charts for extrusion process, *Finite Elements in Analysis and Design*, Vol. 39, pp. 1007-1020, 2003.

[13] B.P.P.A. Gouveia, J.M.C. Rodrigues, N. Bay and P.A.F. Martins, Finite element modelling of cold forward extrusion, *Journal of Materials Processing Technology*, Vol. 94, pp. 85-93, 1999.

[14] K. Srinivasan and P. Venugopal, Warm open die extrusion of TI-6Al-4V, *Journal of Materials Processing Technology*, Vol. 38, pp. 265-278, 1993.

ANALIZA IZGURAVANJA LEGURE Al-5Zn-1Mg KROZ OTVORENI KALUP POMOĆU KONAČNIH ELEMENATA

SAŽETAK

U ovom radu se proučava izguravanje kroz otvoreni kalup legure Al-5Zn-1Mg analizom pomoću konačnih elemenata. Da bi se pronašle odgovarajuće granične vrijednosti mijenjala su se dva osnovna parametra, nagib kalupa i deformacija izguravanja. Analizirano je djelovanje glavnih parametara na izguravanje kroz otvoreni kalup, te su se dobile granice deformacija. Postignuti rezultati su potvrđeni njihovom usporedbom s eksperimentalnim podacima. Zaključeno je da je čisto izguravanje kroz otvoreni kalup moguće do vrijednosti deformacija izguravanja od 0.28 (relativna deformacija za vrijeme izguravanja). Međutim, kako se povećava deformacija izguravanja od 0.09 do 0.28, tako prevladavaju poremećaji preko čistog izguravanja mijenjajući nagib kalupa od 12° do 40°.

Ključne riječi: *izguravanje kroz otvoreni kalup, nagib kalupa, deformacija izguravanja, Al-5Zn-1Mg legura, granična deformacija.*